International Journal of Hydrogen Energy 63 (2024) 207–216

Contents lists available at ScienceDirect

International Journal of Hydrogen Energy

journal homepage: www.elsevier.com/locate/he

Ageing of elastomers in air and in hydrogen environment: A comparative study

M. Zaghdoudi [a], A. Kömmling [b], M. Böhning [b], M. Jaunich [b,*]

[a] Bundesamt für die Sicherheit der Nuklearen Entsorgung (BASE), 10623, Berlin, Germany
[b] Bundesanstalt für Materialforschung und -prüfung (BAM), 12200, Berlin, Germany

ARTICLE INFO

Handling Editor: Suleyman I. Allakhverdiev

Keywords:
Degradation
Thermo-oxidation
Hydrogen
Rubber sealing
Long term exposure
Rapid gas decompression

ABSTRACT

EPDM, HNBR and FKM materials were exposed at 150 °C to air under atmospheric pressure and to hydrogen at 50 bar for different ageing times. All measurements after hydrogen exposure were conducted on samples in degassed condition to assess irreversible effects resulting from that exposure and to compare them to those after ageing in air. Density, hardness, tensile properties, compression set, and hydrogen permeability of all samples were analysed. In both ageing environments, HNBR exhibited the most significant changes of material properties. However, for both EPDM and HNBR, considerably less severe ageing effects were observed under hydrogen in comparison to ageing in air. On the other hand, FKM showed about the same low level of deterioration in both ageing environments but exhibited poor resistance against damage due to rapid gas decompression in hydrogen environment that can lead to seal failure. The obtained results may serve as a guidance toward a better understanding for design and utilisation of elastomeric materials in future hydrogen infrastructure components.

1. Introduction

With the increase in energy demand and the global climate change, a rapid energy transition towards sustainable energy sources is mandatory. In this context, hydrogen is considered one of the most promising energy carrier candidates for the future [1,2]. Hydrogen is an environmentally clean energy carrier that does not emit CO_2 or other harmful substances when burnt.

In the entire hydrogen value chain from generation and storage, transport, and distribution all the way to application, elastomer components are used [3]. They are generally expected to be exposed to a wide range of pressures (up to 875 bar) in combination with a wide range of temperatures (from −40 °C to 200 °C) depending on the operation conditions [4]. Production, storage, transport, and use of hydrogen as a future energy carrier place high demand on the requirements concerning safety, compatibility, and lifetime of the used materials [5–8]. Several studies addressed the issue of elastomer compatibility in high pressure hydrogen [9–11] and the effect of rapid gas decompression (RGD) [12–14]. RGD is caused by a fast pressure decrease acting on a material which was previously saturated with gas under high pressure. As a result of the limited diffusivity of the gas in the material, the desorption might be slower than the pressure release. This leads to the local accumulation of gas, especially at inner surfaces and interfaces (filler/matrix), which expands during the pressure decrease and could form a bubble within the material. If the generated stresses within the material exceed the tear strength, the bubbles cause crack formation and growth and may ultimately destroy the material. To ensure the safety and reliability of technologies featuring rubber materials in hydrogen infrastructure, the effect of the material recipe (filler content and types, plasticizers) was also investigated [12,15,16].

However, in addition to instantaneous damage phenomena such as RGD, it is also necessary to investigate the effect of ageing of rubber materials in hydrogen environment to enable the selection of suitable materials for specific applications and to evaluate the possibility of using existing infrastructure for hydrogen distribution. A recent feasibility study on using gas infrastructure for hydrogen transport in Europe has shown that a 80 bar natural gas pipeline - which represents 80 % of the existing infrastructure [17] - could be converted to a 45–55 bar H_2 pipeline [18]. This is accounted for in this study by choosing 50 bar H_2 pressure as ageing condition. In other papers the addition of hydrogen into the existing natural gas distribution system was addressed [19].

Concerning the degradation of elastomers exposed to gaseous environments, it was recently demonstrated that under pure hydrogen exposure, Ethylene-propylene-diene rubber (EPDM), nitrile butadiene

* Corresponding author.
E-mail address: matthias.jaunich@bam.de (M. Jaunich).

https://doi.org/10.1016/j.ijhydene.2024.03.053
Received 8 December 2023; Received in revised form 28 February 2024; Accepted 4 March 2024

rubber (NBR) and fluorocarbon rubber (FKM) exhibit less degradation in comparison to other gas mixtures [20]. However, at elevated temperatures, accelerated damage mechanisms can be expected [21]. Among the most studied topics in the literature for elastomers is the effect of thermo-oxidative ageing, probably since it is frequently encountered in industrial applications [22]. It is therefore of interest to compare the influence of hydrogen and the well-known thermo-oxidative ageing on behaviour and performance of different elastomers. In previous studies, a comparison of the behaviour of hydrogenated nitrile butadiene rubber (HNBR) in thermo-oxidative environment and other harsh environments has shown a better resistance of thermo-oxidatively aged HNBR against RGD than swollen and virgin HNBR material [21,23]. To the best of our knowledge, the ageing of elastomers at high temperature in hydrogen environment for up to 100 days has not been investigated so far. Most of the conducted research was limited to standard specimens, room temperature and only several weeks of ageing in high pressure (above 800 bar) hydrogen environment at temperatures that did not exceed 110 °C [4]. For example, Fujiwara et al. observed no structural changes in NBR after 40 cycle exposures to 90 MPa hydrogen gas at 30 °C [24]. Hydrogenation of NBR was only noted in the presence of rhodium catalysts [25]. Menon et al. exposed NBR and FKM to high pressure hydrogen (70–100 MPa) under static, isothermal, and isobaric conditions. While the glass transition temperature of NBR did not change, it decreased slightly for FKM [26]. No influence on crack growth behaviour due to high-pressure hydrogen (up to 10 MPa at RT) was observed for unfilled EPDM by Yamabe and Nishimura [27]. Compression set resistance of differently filled NBRs was studied by Simmons et al. [9] by exposing samples to up to 90 MPa of hydrogen gas for 22 h at 110 °C. They postulated that an agglomeration of plasticiser particles and the resulting phase separation can contribute to compression set. On the other hand, long-term thermo-oxidative ageing of elastomers has been extensively investigated [28–30]. In an earlier study in our lab, the degradation - monitored as a change of the mechanical properties as well as sealing ability - of EPDM, HNBR and FKM was studied for up to five years of thermo-oxidative ageing at different temperatures between 75 °C and 150 °C [31]. With an arbitrary end-of-lifetime criterion of 70 % compression set (CS), the estimated lifetimes at 75 °C were 4.5 years, 50 years and 526 years for HNBR, EPDM and FKM, respectively [31]. Hence, of these three investigated materials, FKM was the most ageing resistant, whereas HNBR degraded faster than EPDM. The same materials were now tested in hydrogen environment at a high temperature of 150 °C in order to test the common assumption that the ageing effects in pressurised hydrogen are less severe than in air at atmospheric conditions, since oxygen as the main driver of degradation is not present. However, the increased pressure of 50 bar in hydrogen environment leads to reversible physical effects such as swelling, plasticisation and compression. After removal from hydrogen atmosphere, some time is needed for the hydrogen to diffuse out, and for the polymer and filler network [9] to relax. These circumstances point to the importance of timing when properties of such exposed specimens are to be measured. Therefore, the samples were measured and compared a sufficiently long time after exposure (after at least 48 h) when it was assumed that all hydrogen had diffused out and the samples were again at equilibrium state. This enabled investigating the materials at the same state and comparing only irreversible, permanent degradation effects. In this context, the phenomenon of RGD is a special case where the quick release of the external pressure leads to bubble formation in the suddenly super-saturated polymer matrix, especially at microscopic voids or internal interfaces (filler particles) which may result in a rupture of the material [32]. This is a purely physical phenomenon but leads to irreversible changes or even catastrophic failure. It might be promoted by preceding degradation effects.

It is evident that measurements shortly after removal of the specimen is always experimentally difficult, although it can provide important details of the material behaviour. This is why many standards describing test procedures (such as CSA/ANSI CHMC 2:19 [33], NORSOK M − 710 [34] or ISO 23936–2 [35]) recommend both, immediate measurements as well as an evaluation after 24 h, 48 h or even longer periods of time when the diffusion and relaxation processes can be considered complete. However, as the focus of this paper is the comparison of the long-term ageing effects in the respective media, only measurements on samples in degassed conditions (at least 48 h after removal from hydrogen atmosphere) will be presented.

A first ranking of the materials of the present study from the least resistant to the most resistant in moderate pressure hydrogen (50 bar) at high temperature will be presented and the material performance will be compared to that in a thermo-oxidative ageing environment. The obtained results may serve as a guidance toward a better understanding for design and utilisation of elastomeric materials in future hydrogen infrastructure components.

2. Experimental

2.1. Materials

The investigated materials are standard elastomers from a commercial seal manufacturer of the following rubber types: EPDM, HNBR and FKM. EPDM and HNBR are peroxide-cured, while FKM is bisphenol-cured. The EPDM contains 48 wt% ethylene, 4.1 wt% ethylidene norbornene (ENB) and 90 phr carbon black fillers. The HNBR polymer contains 36 wt% acrylonitrile (ACN) and was reinforced with 80 phr of filler (75 phr carbon black and 5 phr silica). It was softened with 5 phr of plasticiser. The FKM contains 66 % fluorine in the polymer and 70 phr of silica and silica-chalk filler. All materials have an initial Shore A hardness of 80, corresponding to a Shore D hardness of 33. O-rings (as halves or smaller segments) with an unchanged cord diameter of 10 mm and an inner diameter of 190 mm as well as sheet material and standard tensile specimens with a thickness of 2 mm were aged. The O-rings were aged both in a state of 25 % compression and in the uncompressed state. For permeability measurements, membranes with a thickness of 200–300 μm were split from the 2 mm thick sheet material before ageing with a special machine.

With respect to the choice of different specimens regarding size and geometry one should keep in mind that consideration of a broad range of properties and corresponding testing methods was the priority for the design of the aging exposure – of course in combination with a strongly limited space available in the autoclave. Rather than preparing different specimens from a single bulk sample it was chosen to directly expose specimen of the required geometry because ageing the samples could cause embrittlement which would impede sample preparation. This does not exclude possible differences in the individual aging processes; however, the assessment of aging effects is in any case based on comparing the same property before and after aging exposure.

2.2. Ageing

Ageing was performed in two different atmospheres (hydrogen at 50 bar and air at ambient pressure) at 150 °C. The ageing times were planned to be 10 d, 30 d and 100 d, however, 1 or 2 d deviations occurred for some samples. The actual exposure times are indicated in the respective figures.

2.2.1. Thermo-oxidative ageing

Samples were aged in air-circulating ovens at 150 °C up to 101 d. For measuring the compression set, two half O-rings of each material were aged compressed by 25 % between stainless steel plates. The uncompressed O-rings and segments with a cord diameter of 10 mm as well as the sheets, membranes and standard tensile specimen with a thickness of 2 mm were aged in a stress-free state.

2.2.2. Ageing in hydrogen

The ageing in hydrogen (H_2) at 50 bar and 150 °C for a storage period

of up to 99 d was conducted in a remotely monitored and controlled 6 l autoclave (Fig. 1(a)) with electric heating (Fig. 1(c)). Because the autoclave has limited useable volume and opening diameter, a sample holder has been devised for fitting all samples into the autoclave (Fig. 1 (b)). The compressed O-ring parts were mounted between the three lower thick plates, while the other samples lay on different levels of punched stainless-steel plates. The same sample geometries as described for thermo-oxidative ageing were placed in the sample holder and inserted in the autoclave (Fig. 1 (c)). Before filling and pressurising with hydrogen (H_2), the autoclave was evacuated and filled with nitrogen (N_2) for the first 24 h. This was done to remove residual oxygen, to avoid the formation of an explosive hydrogen-oxygen mixture and to verify the tightness of the pressure vessel. After that, the autoclave was again evacuated and then pressurised stepwise with hydrogen while heating the autoclave until a pressure of 50 bar and a temperature of 150 °C were reached. This filling and heating procedure took about 2 h. The temperature and the pressure were monitored and controlled during the whole storage period. At the end of the storage period, the autoclave was cooled down to room temperature within ca. 22 h a day before. During cooling the pressure decreased from 50 to 36 bar. Finally, the samples were depressurised within 80 min and specimens were removed for characterisation tests. Thus, the samples were exposed to 50 bar hydrogen for 10 d, 30 d and 100 d, but only 9 d, 29 d and 99 d to hydrogen and 150 °C. The latter storage period at the combined exposure was used for comparison with the samples aged under thermo-oxidative conditions.

3. Methods

Characterisation tests were performed with up to five specimens per exposure condition for all materials. In the Results section, the mean values or in the case of tensile tests median curves are shown, respectively. The measurements were performed before exposure and at least 48 h after exposure when the H_2 gas content and corresponding material relaxation state of the samples was assumed to be equilibrated (i.e., after desorption of the major part of it) [36], which allows assessing the irreversible ageing effects. While major investigations in H_2 were conducted after short time after exposure (20 min–30 min according to the standard CSA/ANSI CHMC 2:19 [33]) to assess the physical property changes in the gas swollen condition the present investigation focuses on irreversible changes in degassed conditions as explained in the introduction. For compression set tests, samples were kept compressed in the sample holder for 2 h after removal from the autoclave. After that, measurements were performed at different times after disassembly, the first one after 30 min. This 30 min CS measurement in the only case when samples where measured before 48 h degassing time.

Density measurements were performed on rectangular samples (10 mm × 10 mm) with a thickness of 2 mm according to ASTM D 792 [37]. Two samples were measured and the mean value is given. The weight of the samples was measured in air (m_{air}) by means of a Mettler Toledo balance with an accuracy of 10^{-4} g. After that, the samples were immersed in water and the weight in water (m_{water}) was determined. The specimen density (ρ) is calculated from Eq. (1):

$$\rho = \frac{m_{air}}{m_{air} - m_{water}} \bullet (\rho_{water} - \rho_{air}) + \rho_{air} \quad (1)$$

Hardness measurements were conducted using Shore D hardness (DIN EN ISO 868 [38]) with an indentation time of 3 s (Note that in view of the expected increase in hardness (>80 Shore A) Shore D was chosen instead). For samples aged in H_2 environment, the tests were carried out on the shoulders of the tensile specimens that were stacked to give a sample height of 6 mm. Nine stacks were measured, and the average value is given. For samples aged in thermo-oxidative environment, hardness measurements were performed on 2 mm sheet material that was also stacked to give a sample height of 6 mm.

For the tensile experiments dumbbell specimens (type S2 from DIN 53504 [39]) were punched out of plates with a thickness of 2 mm before exposure. All the tests were performed with a Zwick universal testing machine with a 5 kN load cell and a deformation rate of 0.1/s (238 mm/min) at standard temperature (23 ± 2 °C). Three to five specimens were used per test.

Compression set (CS) provides information about the O-ring's resilience and therefore indirectly about the sealing performance. While most studies on elastomers in H_2 environment have been performed on laboratory samples that have been compressed for a limited time after storage, the current study deals with O-rings that were in the compressed state continuously during hydrogen storage, which corresponds to the assembly situation in the application. CS is calculated from Eq. (2) where h_0, h_1 and h_2 are respectively the initial, the compressed and the recovered height of the sample.

$$CS(t) = \frac{h_0 - h_2(t)}{h_0 - h_1} \bullet 100\% \quad (2)$$

Ten positions on each half O-ring were measured at the respective time after removal from the ageing environment and the average values are analysed. Samples that were aged in H_2 environment were left for 2 h in compressed state after removal from the autoclave. Samples that were

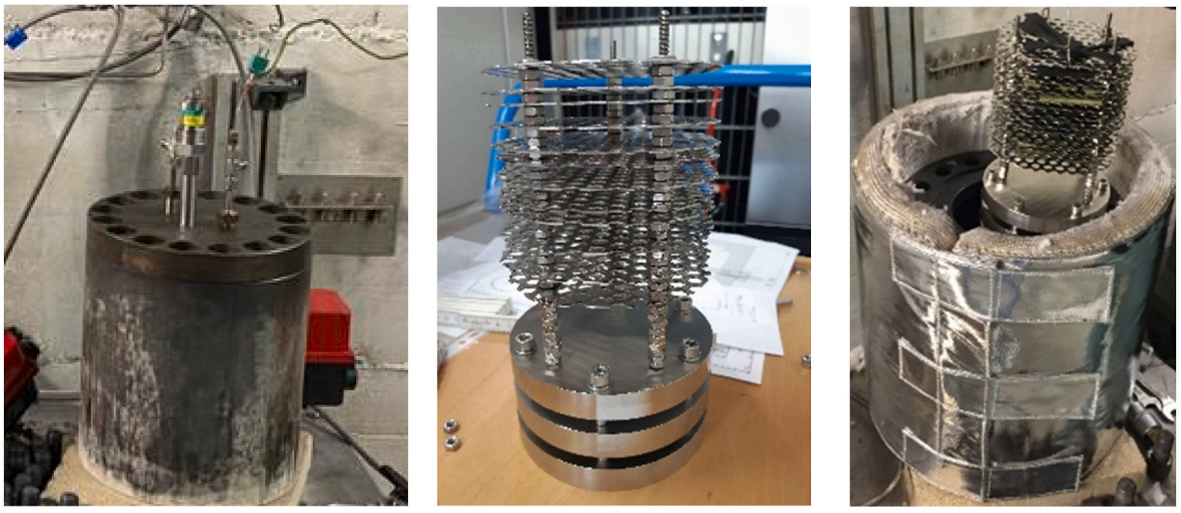

Fig. 1. (A) 6 l autoclave, (b) developed sample holder, (c) 6 l autoclave (with installed electric heating) with the developed sample holder being removed.

aged in thermo-oxidative environment were taken from the ageing oven at a given ageing time and left compressed during cooling to room temperature. According to standards ASTM D395 [40] and DIN ISO 815–1 [41], the recovered height h_2 is measured after 30 min. As CS is time dependent, the recovered height h_2 was also measured after 5 d. To reach an equilibrium CS value, an additional tempering was applied [42]. The respective O-ring pieces were placed for 1 d in an oven at 100 °C after which the recovered height h_2 was measured again [32].

Gas permeability measurements with H_2 were conducted on circular samples with a diameter of 20 mm. The samples were die cut from 200 to 300 μm thick membranes that were aged in the given environment together with the other samples. The reduced thickness of the membrane was required to ensure a reasonable measurement time of the permeation test. The permeability measurements were performed using a constant volume variable pressure set-up following the time-lag method. Therefore, the samples were degassed thoroughly prior to the measurement with a turbomolecular vacuum pump system ($p < 10^{-6}$ mbar) until no outgassing of residual volatile compounds could be detected, which took up to four days. After applying the upstream gas pressure (1 bar), the pressure increase in the evacuated downstream volume was recorded using a capacitance manometer (MKS Baratron 631C, 10 mbar range) temperature controlled at 100 °C. The sample cell and gas reservoir were placed in an air temperature-controlled housing. The temperature of 35 °C was held constant (± 0.2 K) by permanent cooling and controlled heating (regulated by a Eurotherm 3204 temperature controller). The permeability coefficients P were determined from the slope of the time-dependent downstream pressure increase in the steady state, whereas the diffusion coefficients D were obtained from the time-lag τ determined by extrapolation of the steady-state curve to the time axis (p = 0) according to eq. (3)

$$D = \frac{\ell^2}{6\tau} \tag{3}$$

with ℓ beeing the thickness of the tested sheet. As the film is completely degassed prior to the measurement (penetrant concentration c = 0) the time necessary to reach the steady state with respect to permeability represents the establishing of a constant penetrant concentration gradient across the membrane which is determined by the diffusion coefficient and therefore allows its calculation according to eq. (3).

As the investigated elastomers are nonporous ('dense') polymeric materials, the gas transport is based on the solution-diffusion mechanism. Thus, the permeability P is defined as a product of the diffusivity D and the solubility coefficient S of the penetrant gas:

$$P = D \cdot S \tag{4}$$

The permeability coefficients P are determined as:

$$P = \frac{Q \bullet \ell}{A \bullet t \bullet \Delta p} \tag{5}$$

(Q – amount of permeated gas expressed as volume at STP, A – membrane area, Δp – pressure difference between upstream and downstream side).

P is expressed in Barrer in this paper which is defined as:

$$1\ Barrer = 10^{-10} \frac{cm^3\,(STP)\ cm}{cm^2\ s\ cmHg}$$

Where STP refers to the standard temperature (273,15 K) and the standard pressure (1 bar) conditions.

4. Results and discussion

In order to characterise differences in the ageing behaviour of the investigated elastomer materials under thermo-oxidative conditions and in hydrogen atmosphere, changes in relevant properties were determined after different exposure times, as elaborated in the following chapters. At the end the materials are compared with respect to their overall performance.

4.1. Density

For a better comparison of the relative changes, the density was normalised with respect to the value of the unaged sample. Fig. 2 shows the normalised density of EPDM, FKM and HNBR aged at 150 °C for different ageing times in air and in hydrogen at 50 bar. For EPDM and HNBR samples aged in air, a clear increasing trend with ageing time is observed. This increase is more pronounced for HNBR. For FKM the density remains almost the same. On the other hand, for all materials aged in hydrogen environment, no clear trend over ageing time can be observed, as only minor changes occur.

For thermo-oxidative ageing, the observed density increase could be related to different factors. One among them is crosslinking, that can also lead to shrinkage [43] and thus densification. As HNBR contains 5 phr of plasticizers, in this case the increase in density could also be due to plasticiser loss. On the other hand, all investigated materials contain high-density fillers (e.g. carbon black, density ~1.8 g/cm^3, and silica, density ~2.6 g/cm^3). Therefore, a reduction of the lower density polymer component by loss of volatile degradation products would increase the relative contribution of the higher density fillers, and consequently the density can increase [43]. Another factor that affects density increase at later ageing stages is the insertion of heavier oxygen atoms (as hydroxyl or carbonyl groups) that results from oxidative chain scission reactions. However, for hydrogen aged samples only differences of max. ± 1 % were found. As the density does not change notably here, this confirms the expectation that the above-mentioned degradation effects under thermo-oxidative do not play a significant role for ageing under hydrogen at the given ageing conditions.

4.2. Hardness

Fig. 3 presents the hardness results of EPDM, FKM and HNBR aged in hydrogen and in air. While HNBR and EPDM samples aged in air exhibit increasing hardness with increasing ageing time, the hardness remains basically unchanged for all three materials when aged under hydrogen, with only a slight increase for HNBR and FKM aged for the longest period of 99 d. However, when the hardness values of samples aged in hydrogen are compared to those of the unaged samples, the hardness after hydrogen exposure remains lower than that of the unaged ones for

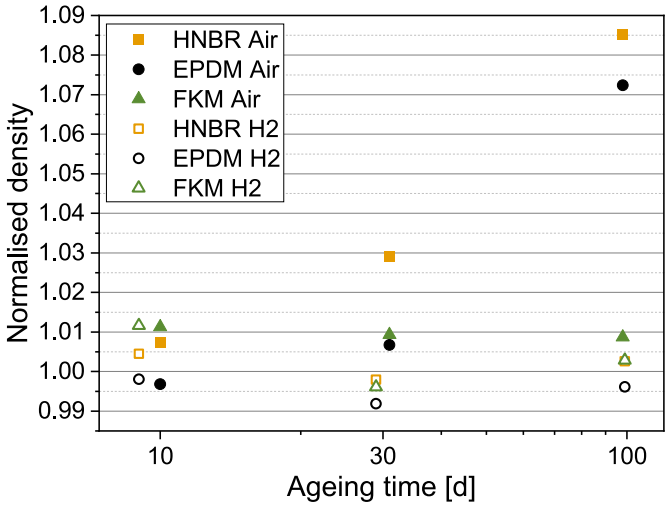

Fig. 2. Normalised density of EPDM, FKM and HNBR aged at 150 °C for different ageing times in air and in hydrogen (with an initial density of 1.16 g/cm^3, 2.09 g/cm^{3}and 1.23 g/cm^3, respectively).

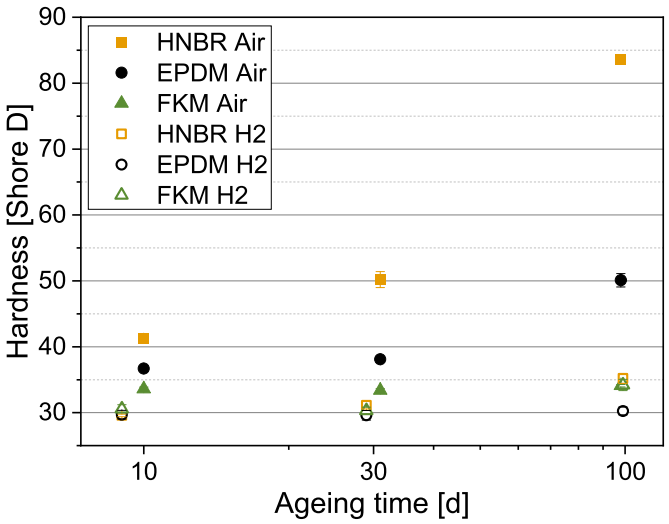

Fig. 3. Hardness results of EPDM, FKM and HNBR aged at 150 °C for different ageing times in air and in hydrogen.

all materials up to 29 d. For the longest period of 99 d, the hardness value of EPDM after ageing in hydrogen is still lower than that of the unaged one. Probably, the hydrogen-induced swelling broke up some bonds between matrix and filler, resulting in lower reinforcing interactions [9,24].

For thermo-oxidatively aged samples, hardness increase could again result from crosslinking and/or plasticiser evaporation. HNBR contains (a small amount of) plasticiser. During thermo-oxidative ageing of the same HNBR it was confirmed in a previous study that crosslinking dominates chain scission [44]. Thus, HNBR exhibited the highest hardness increases during thermo-oxidative ageing also in our present study. For EPDM on the other hand, chain scission and crosslinking occur simultaneously during thermo-oxidative ageing and evolve with the same impact at the early stage of degradation, resulting in a slower hardness increase compared to HNBR. Only at later degradation stages does crosslinking dominate chain scission [44].

Similar to the results obtained from density measurements, the mechanisms responsible for the hardness increase during thermo-oxidative ageing do not seem to play a significant role during ageing in hydrogen, where the hardness hardly changes.

4.3. Tensile properties

Fig. 4 shows the median tensile stress strain curves of the studied materials aged in hydrogen and in air at 150 °C for different ageing times. From Fig. 4, one can see that the thermo-oxidative ageing affects the mechanical response of EPDM and HNBR more strongly compared to H_2 ageing. On the other hand, the opposite effect is observed for FKM (Fig. 4 (c)).

A detailed comparison of the mechanical properties is given in Fig. 5 based on elongation at break, tensile strength, and modulus at 50% elongation (M 50) as indicators. For EPDM aged in air, a decrease of elongation at break and tensile strength, and an increase of the M 50 is observed with increasing ageing time. This could indicate the development of a heterogeneous network structure that can form as a result of both crosslinking and chain scission [45]. On the other hand, for the EPDM exposed to ageing in hydrogen, no clear trend regarding the ageing time can be observed for elongation at break and tensile strength. However, a decrease of the normalised M 50 over ageing time (Fig. 5 (c)) is obtained after a considerable increase in 50 % modulus for the 9 d sample.

For HNBR aged in air, the tensile strength increases simultaneously with decreasing strain at break. This indicates an embrittlement due to dominant crosslinking reactions during thermo-oxidative ageing of HNBR [46]. For the ageing in hydrogen, a slight decrease of both elongation at break and tensile strength was found, while the stiffness at

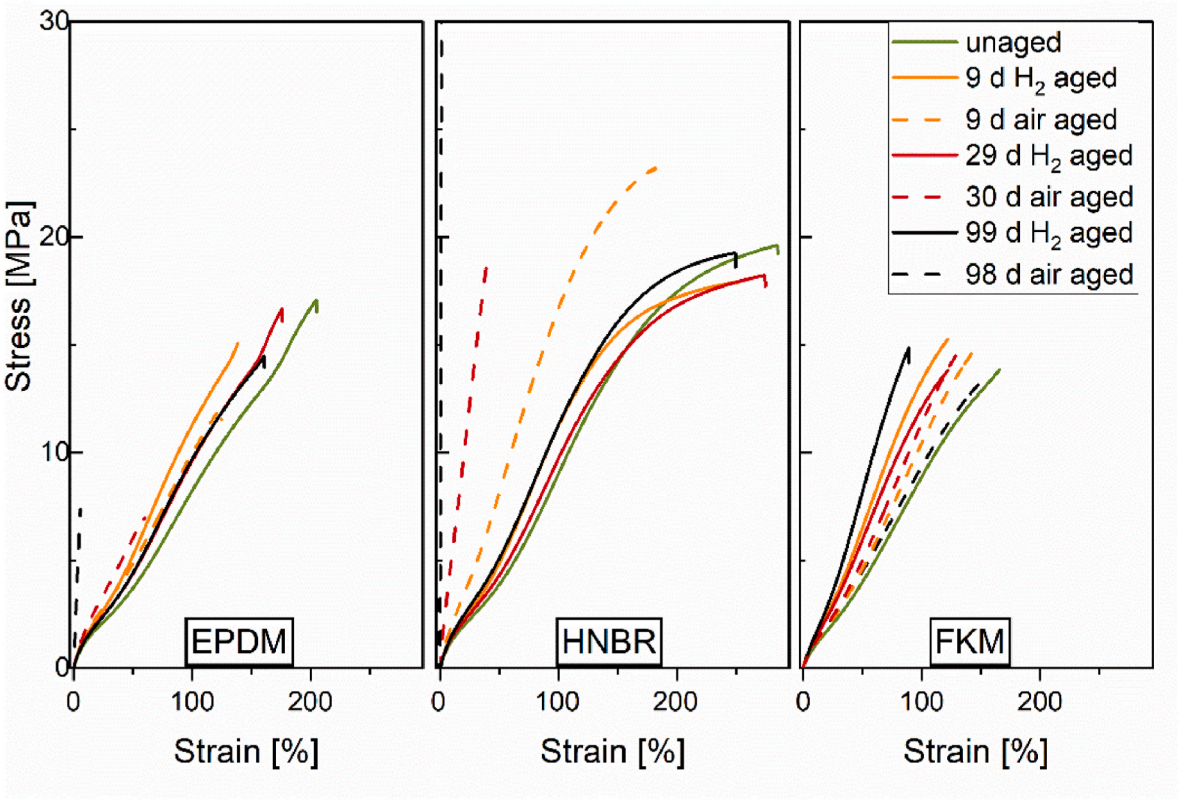

Fig. 4. Tensile stress-strain curves of (a) EPDM, (b) HNBR and (c) FKM aged in air and in H_2 environment at different ageing times.

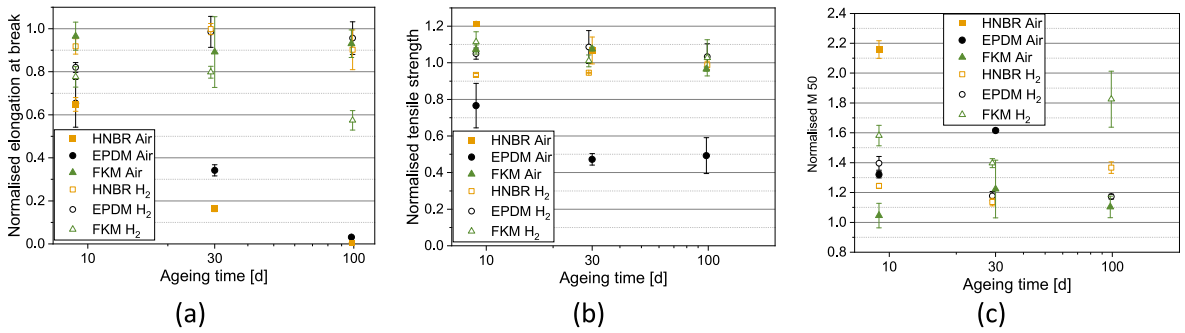

Fig. 5. Normalised (a) elongation at break, (b) tensile strength and (c) modulus at 50 % elongation (M 50) of EPDM, HNBR and FKM aged in air and in H_2 environment at different ageing times. Some values in (c) in air are missing due to premature breakage (see Fig. 4).

higher strains increased slightly compared to the unaged value. Similar to the results of EPDM aged in H_2, no clear ageing trend over time is observable, indicating that no strong systematic changes of the material structure occur during ageing in H_2 at 50 bar and 150 °C.

For FKM aged in air, no significant change of the tensile behaviour was found. Compared to EPDM and HNBR, FKM aged in air exhibits the best ageing resistance under these conditions. However, for the ageing in hydrogen, an increase of the stiffness accompanied with a decrease in the elongation at break is observed in comparison to the unaged samples. Even though the stiffness of the samples aged for 9 d is higher than that aged for 29 d, a trend over ageing time can be observed which combines a higher stiffness/modulus with lower elongation at break. This embrittlement of the material could be due to crosslinking reactions and/or filler matrix interaction changes during ageing at high temperature in H_2 [9,24].

4.4. Compression set

Results of compression set (CS) are shown in Fig. 6 for measurements after 30 min, after 5 d and after additional tempering. While the samples measured after 5 d and after tempering are assumed to contain no residual hydrogen and any possible swelling has relaxed, in the sample measured 30 min after disassembly (which was 2 h after removal from H_2 atmosphere), some hydrogen-induced swelling could still be present, leading to a higher volume which affects the measured height and a softer and probably more flexible material behaviour resulting in lower measured CS data. It should be noted that the relaxation of the swelling is expected to be slower than the actual hydrogen desorption by diffusion.

According to the standards ASTM D395 [40] and DIN ISO 815–1 [41], CS is determined 30 min after release from compression, which is displayed in Fig. 6(a). For thermo-oxidative ageing, EPDM and HNBR exhibit a considerable CS increase with increasing ageing time. (Note that all thermo-oxidative HNBR CS values are affected by DLO effects [47], i.e. the O-ring specimen are not fully and homogeneously aged through the whole bulk due to limited oxygen access in the core material. Thus, the non-DLO-affected values would lie considerably higher especially after 31 and 101 d ageing time, above the points of EPDM aged in air.) On the other hand, for ageing under H_2, the CS values are much lower for HNBR and especially for EPDM, indicating considerably less degradation of the polymer network structure by chain scission and crosslinking. By contrast, FKM exhibits basically the same CS values regardless of the ageing atmosphere. This suggests that the underlying degradation mechanisms are independent of oxygen and possibly a pure effect of temperature and time. Note that under hydrogen ageing, the CS values of EPDM are even below those of FKM, which was assumed to be the most stable material of the three materials based on the results after ageing in air [31], suggesting a very good high-temperature stability of EPDM in hydrogen.

As CS is a time-dependent property, the recovery continues. When CS is measured again after 5 d as shown in Fig. 6(b), all values have dropped, with CS decreases between a few and up to 20 %. No systematic differences between both ageing media can be observed for this recovery step. When applying subsequent tempering to speed up the recovery towards equilibrium, which represents only the effects of irreversible chemical degradation, a further reduction of CS values is observed, as shown in Fig. 6(c). While only little changes between measuring after 30 min and after 5 d were observed for CS values of EPDM aged in H_2, the tempering step led to a significant reduction, resulting in very low CS values. This could mean that beside entropy-elastic recovery, other effects that are temperature-activated could play a role here.

It should be noted that while hardness, density and tensile tests often did not show a clear ageing trend especially under hydrogen, all CS measurements revealed a clear increase with ageing time, indicating that CS measurements are more sensitive to degradation. Additionally,

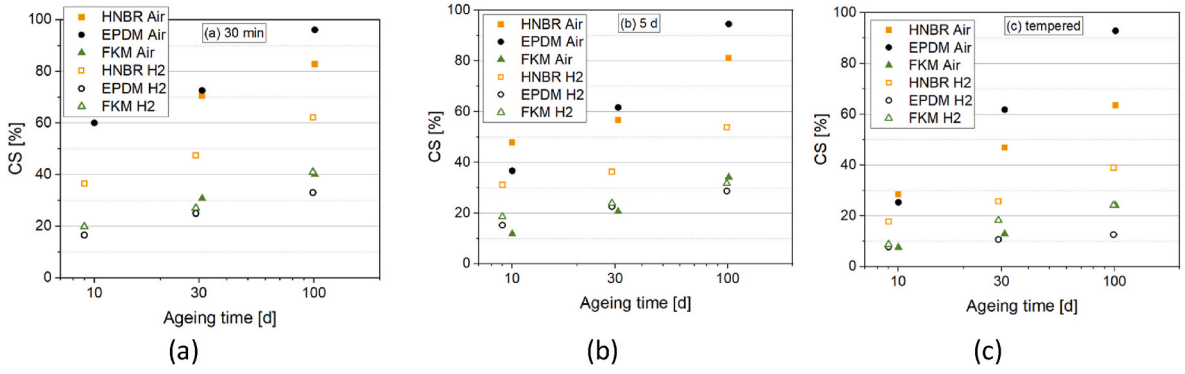

Fig. 6. CS results of HNBR, EPDM and FKM aged in hydrogen and in air after (a) 30 min, (b) 5 d and (c) additional tempering. For HNBR all CS measurements in air are DLO affected.

ageing the samples in the compressed state corresponds to the actual service conditions. This emphasises the benefits of using this CS method.

However, despite the low CS value of FKM in hydrogen environment, the O-ring part that was aged compressed by 25 % for 99 d presented cracks that are typical for rapid gas decompression (RGD) as shown in Fig. 7. The cracks were observed directly when the samples were demounted from the compression plates. Such ascertainments were also reported in Ref. [48] where FKM showed the least amount of deterioration but poor decompression resistance.

At both ends of the O-ring segment, two cracks that are parallel to the loading direction (compression) with lengths of 7 mm and 6 mm, respectively, were observed and are shown in Fig. 8. Beside the above-mentioned cracks, a radial crack of 4 mm length (see Fig. 8(a))) was found at the outer curved surface of the compressed O-ring segment.

The ranking criteria according to NORSOK Standard M − 710 [34] and DIN EN ISO 23936–2 [35] testing standards range between 0 and 6. The best rating is 0 where no internal cracks, holes, or blisters of any size are detected. Ratings of 4 or higher indicate failure. Applying these criteria for the compressed FKM O-ring part results in rank 3 (i.e. there are less than 9 internal cracks of which max. 2 cracks can have a length between 50 % and 80 % of the cross section), indicating a acceptable material behaviour. Note that only a quarter O-ring segment was investigated here, potentially resulting in a lower number of cracks compared to a full O-ring. Additionally, the test pressure according to NORSOK and DIN EN ISO 23936–2 is significantly higher than in the conditions used in the present study. Moreover, the above-mentioned standards do not consider 100 % H_2 gas exposure and require that the suitability of rating 3 has to be evaluated and confirmed for the respective actual application.

Damage from RGD is more likely when the pressure decrease rate is high [13]. This is not the case for the present study. On the other hand, crack damage is only seen for FKM O-ring aged in hydrogen up to 99 d in compressed state. The O-rings that were aged in stress free configuration presented no visible cracks at the same ageing state. On the one hand, this could be because the maximum length of diffusion paths is longer in the compressed and deformed sample, and the free surface is considerably lower due to the contact to compression plates. On the other hand, the mechanical loading in the compressed state could accelerate the formation and propagation of cavities and cracks [49]. RGD is related to the transport properties (solubility and diffusivity) as well as to the mechanical properties of the material. Thus, permeability and diffusivity of EPDM, HNBR and FKM aged in air and in hydrogen will be investigated in the following section.

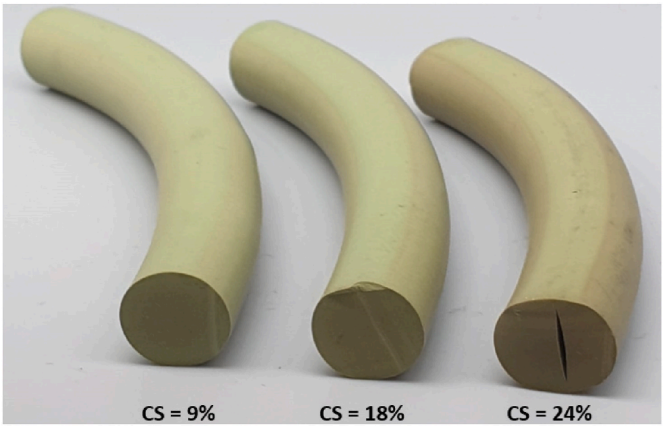

Fig. 7. FKM O-ring parts aged in compression at 50 bar hydrogen and 150 °C for 9 d, 29 d and 99 d and their CS values after tempering. The sample aged for 99 d exhibits cracks.

4.5. Hydrogen permeability

Hydrogen permeability measurements were conducted on membranes aged in hydrogen and in air (Fig. 9). Among the unaged materials, EPDM exhibits the highest hydrogen permeability and FKM the lowest. During ageing in H_2, the permeability of the materials remains basically constant, while it decreases for EPDM and HNBR during thermo-oxidative ageing, probably due to crosslinking. Permeability is dependent on free volume which could be roughly related to a material's density [50]. While FKM exhibits the highest density of 2.09 g/m^3 and also the lowest permeability, such a simplified relation does not apply for EPDM and HNBR, which have somewhat similar densities of 1.16 g/m^3 and 1.23 g/m^3, but EPDM has considerably higher permeability. This reflects the more complex permeation mechanism of solution diffusion (as detailed below) but is also a consequence of rubbers being complex materials made of different polymers, other organic compounds and fillers, each with their respective influence on permeability.

According to the solution-diffusion mechanism, permeability P is the product of diffusivity D and solubility S (Eq. (4)). Thus, further insights can be gained by evaluating diffusivity results which can be directly obtained by the permeation measurement using the time-lag method. Therefore, diffusivity results are shown in Fig. 10. Unaged EPDM presents the highest diffusivity for hydrogen. In general, the diffusivity depends on the cohesive energy of the polymeric matrix, i.e. the cohesive forces per unit of length of the chain [51]. In terms of the solution-diffusion mechanism, this determines the energy required to open a transient pathway (bottleneck) to allow a translational "jump" of a penetrant molecule as the basic step for diffusional transport. Polar groups within the polymer structure significantly increase these cohesive forces due to stronger intermolecular van der Waals interaction. As a consequence, gas molecules may exhibit distinctly lower diffusivities in such polymer matrices, which can be nicely seen from comparison of respective elastomers [52–54]. This is also the case for HNBR containing nitrile groups exerting strong polar intermolecular interactions between polymer chains. On the other hand, EPDM which is non-polar therefore shows a higher diffusion coefficient for hydrogen. However, chain packing, and the resulting free volume of the polymer matrix (FFV – fractional free volume) also affect diffusivity and solubility as the underlying properties of permeability. The interchain spacing in the amorphous structure of the polymer determines the extend of motion or deformation needed to overcome the bottleneck and form the diffusion pathway and therefore also the required energy and thus diffusivity and the corresponding activation energy. On the other hand, besides specific interactions between gas and polymer, the free volume (the void space between the polymer chain molecules) largely determines the amount of gas which can be taken up, i.e. the solubility. In this context FKM, the material with the highest density also shows the lowest FFV [55] and the lowest gas uptake, and thus in combination with the lowest diffusivity also the lowest permeability. Furthermore, in this discussion it has to be taken into account that the investigated rubber material does not consist of the polymer matrix alone but contains a number of additives and fillers. Especially for the latter the interfacial properties may have a decisive influence on the overall mechanical properties as well as the gas transport behaviour. For the fluorinated FKM also weak interactions must be expected – with respect to the cohesive forces of the matrix itself as well as with respect to the interaction with the filler. This is the reason why, compared to the other two elastomers, FKM shows the strongest tendency to damages by rapid gas decompression (RGD) – see section above. Although there is no obvious simple structure-property relation, the results obtained for the investigated elastomer materials reflect the respective dominating influence of cohesive/interfacial forces and the FFV. The non-polar EPDM clearly shows the highest diffusion coefficients and permeabilities, whereas the polar HNBR exhibits distinctly lower diffusivities and also permeabilities. The potentially stronger interaction within the matrix and with filler particles reduce the tendency of RGD failure. In contrast to that FKM combines low diffusivities

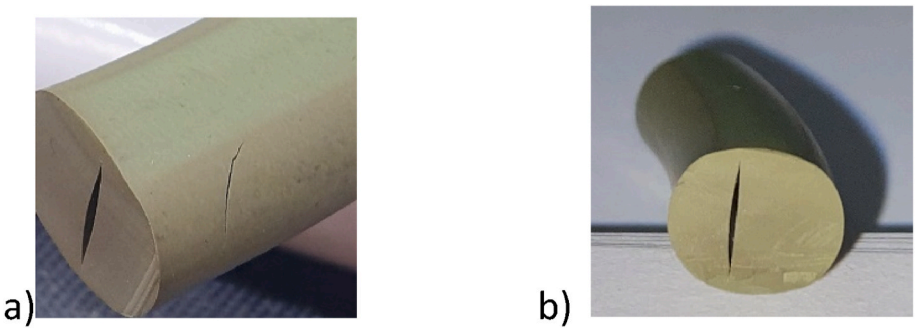

Fig. 8. Cracks formed at both ends of the FKM O-ring segment.

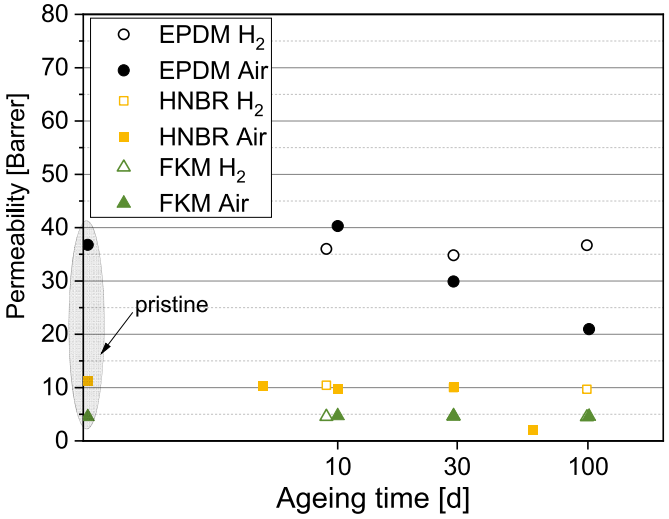

Fig. 9. H_2 permeability results. The HNBR sample after 100 d of ageing in air at 150 °C was too brittle for measuring. The points for air and H_2 overlap for HNBR and FKM aged for 29 d as well as for FKM aged for 100 d.

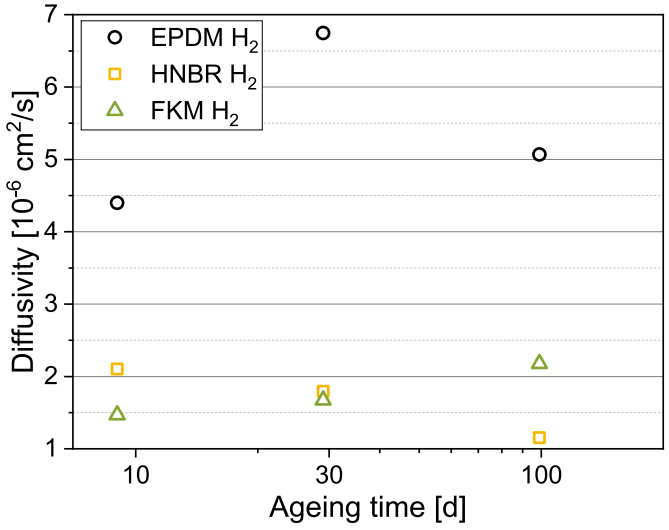

Fig. 10. H_2 diffusivity results.

and permeabilities with only weak interactions of the elastomeric matrix material, making it more sensitive to damages by RGD. During ageing in H_2, the diffusivity for EPDM and FKM increases with increasing ageing time while it decreases for HNBR.

For seals in the hydrogen infrastructure, a low hydrogen permeability is beneficial for minimizing H_2 gas loss in the system. On the other hand, low diffusivity can also lead to RGD and seal failure, as observed for FKM.

In the context of RGD the underlying material cavitation is influenced by hydrostatic stress components. Gent et al. [56,57] developed a mechanical cavitation model that related the critical hydrostatic pressure Π_c that is required for the initiation of cavitation damage to the young's Modulus E of the material (Eq. (6))

$$\Pi_c \geq \frac{5E}{6} \tag{6}$$

This means that if a gas bubble exists, it might serve as a starting point of blister initiation in the rubber, if the initiation limit pressure of the blister (i.e. the critical hydrostatic pressure) is of the order or greater than the material's Young's modulus. Under the actual exposure conditions used in this study, the tensile properties changed in comparison to the virgin material (Figs. 4 and 5) indicating that the thermal effect which induces mechanical property changes plays an important role. Even though no Young's modulus could be determined in this study, the normalised modulus at 50 % elongation (M50) was evaluated as can be seen in Fig. 5 (c) and increased by 60 % after 9 d of ageing in hydrogen for FKM and by 40 % after 29 d with no formation of visible cracks. However, between 60 % and 80 % increase, several cracks were identified. Even though the modulus increased, which increased the critical pressure threshold according to eq. (6), cracks were forming. A possible reason could be the reduced normalised elongation at break of FKM after ageing in hydrogen environment. After 99 d, it is about 40% lower than the unaged one (Fig. 5 (c)), which could indicate reduced tear strength.

Besides the effect of mechanical property changes, cavitation of elastomers under the present conditions is generally induced due to decompression after gas saturation. For blister formation after decompression, the internal pressure Π is proportional to the concentration c of the gas dissolved in the rubber and is expressed as [58]:

$$\Pi = \frac{c}{S} \leq p \tag{7}$$

Where S is the solubility (defined in Eq (4)) and p is the exposure pressure (50 bar).

As shown in Fig. 10, the diffusivity of FKM is smaller than that of EPDM and HNBR and increases only slightly with increasing the exposure time. This means that the desorption of the dissolved gas is slower which results in higher internal pressure Π.

Even under normal operating conditions (e.g. in pipelines), where no sudden pressure drops resulting in RGD effects at the seals should occur, the effect of temperature and exposure time should not be neglected- With the increase of operating pressure and temperature, more severe damage is to be expected [59,60]. Moreover, if a crack is present and the stress is sufficiently high, the crack growth in rubber is progressive with time during constant loading. So the longer the loading time the further the crack propagates [58].

4.6. Material comparison

The effect of temperature at relatively low hydrogen pressure (50 bar) in this study has barely shown changes in hardness and normalised density over ageing time (Figs. 2 and 3) for the three investigated materials and almost the same values for HNBR and FKM at 29 d and 99 d. Changes in tensile properties of EPDM aged at 9 d are comparable to those of FKM at 99 d (Figs. 4 and 5). Furthermore, EPDM exhibited the best stability with regard to compression set (Fig. 6), which is the most relevant property for seals investigated in this study. HNBR showed the highest compression set. FKM exhibited only moderate changes in the tested material properties indicating a high degradative stability but low resistance against damage due to rapid gas decompression. Even if normalised density and mechanical properties of FKM aged at 99 d are comparable to HNBR and EPDM at other ageing times, transport properties are crucial to understand seal failure due to RGD and subsequent crack formation. While both EPDM and FKM exhibited very good ageing resistance in their mechanical properties under the tested hydrogen environment, EPDM exhibited quite high hydrogen permeability, possibly resulting in H_2 losses if used in H_2 infrastructure, and FKM was sensitive to RGD, though this is only an issue in applications where sudden pressure drops can occur. However, as the use of fluorinated polymers will possibly be restricted in the future, the search for compatible polymers should continue.

Structural changes that induce mechanical property changes during ageing in hydrogen at high temperature will be investigated and analysed in the future work.

5. Conclusion

Degradation of EPDM, HNBR and FKM at 150 °C in air and in hydrogen after exposure times up to 100 d was investigated. On the basis of density, hardness, tensile test, compression set and permeability results of the aged and degassed material, the materials could be classified according to their ageing resistance in each ageing environment. For the materials aged in air FKM exhibited the best performance, and EPDM presents better stability than HNBR. For ageing in hydrogen environment, EPDM showed the least degradation, and HNBR the most. Even though FKM presented good mechanical properties after ageing, it also developed tears/cracks, indicating poor decompression resistance. On the other hand, EPDM exhibited the highest hydrogen permeability which might be critical for the seal tightness when used in hydrogen infrastructure. However, due to the large variety of rubber compounds and fillers, further tests need to be performed with other material formulations and ageing conditions with regard to the specific application and the operating long-term conditions. Additionally, systematic studies addressing cohesive properties of the elastomeric matrices (as e.g. tear strength) as well as the interface to various fillers and their effect on diffusivity and solubility of hydrogen are desirable for a better understanding.

Based on the obtained results, we can conclude that the choice of a suitable elastomer material for sealing in hydrogen applications is an assessment of the subtle balance between (1) resistance against ageing and long-term performance, (2) diffusivity and permeability as well as (3) the tendency to blister formation, crack propagation and resistance against rapid gas decompression failure.

Declaration of competing interest

The authors declare that they have no known competing financial interests or personal relationships that could have appeared to influence the work reported in this paper.

Acknowledgements

The authors want to thank their colleagues T. Rybak, D. Schulze and V. Reimer for permeability, hardness and tensile measurements and E. Askar for performing the hydrogen aging of the samples.

References

[1] Madadi Avargani V, Zendehboudi S, Cata Saady NM, Dusseault MB. A comprehensive review on hydrogen production and utilization in North America: prospects and challenges. Energy Convers Manag 2022;269:115927.
[2] Incer-Valverde J, Patiño-Arévalo LJ, Tsatsaronis G, Morosuk T. Hydrogen-driven Power-to-X: state of the art and multicriteria evaluation of a study case. Energy Convers Manag 2022;266:115814.
[3] Zheng Y, Tan Y, Zhou C, Chen G, Li J, Liu Y, et al. A review on effect of hydrogen on rubber seals used in the high-pressure hydrogen infrastructure. Int J Hydrogen Energy 2020;45:23721–38.
[4] Balasooriya W, Clute C, Schrittesser B, Pinter G. A review on applicability, limitations, and improvements of polymeric materials in high-pressure hydrogen gas atmospheres. Polym Rev 2021:1–36.
[5] Rivkin C, Burgess R, Buttner W. Hydrogen technologies safety guide. ; national renewable energy lab. (NREL). Golden, CO (United States). 2015. p. 73. p. Medium: ED; Size.
[6] Conte M, Prosini PP, Passerini S. Overview of energy/hydrogen storage: state-of-the-art of the technologies and prospects for nanomaterials. Mater Sci Eng, B 2004; 108:2–8.
[7] Moradi R, Groth KM. Hydrogen storage and delivery: review of the state of the art technologies and risk and reliability analysis. Int J Hydrogen Energy 2019;44: 12254–69.
[8] San Marchi C, Hecht ES, Ekoto IW, Groth KM, LaFleur C, Somerday BP, et al. Overview of the DOE hydrogen safety, codes and standards program, part 3: advances in research and development to enhance the scientific basis for hydrogen regulations, codes and standards. Int J Hydrogen Energy 2017;42:7263–74.
[9] Simmons KL, Kuang W, Burton SD, Arey BW, Shin Y, Menon NC, et al. H-Mat hydrogen compatibility of polymers and elastomers. Int J Hydrogen Energy 2021; 46:12300–10.
[10] Fujiwara H, Ono H, Nishimura S. Effects of fillers on the hydrogen uptake and volume expansion of acrylonitrile butadiene rubber composites exposed to high pressure hydrogen: -Property of polymeric materials for high pressure hydrogen devices (3). Int J Hydrogen Energy 2022;47:4725–40.
[11] Fujiwara H, Ono H, Ohyama K, Kasai M, Kaneko F, Nishimura S. Hydrogen permeation under high pressure conditions and the destruction of exposed polyethylene-property of polymeric materials for high-pressure hydrogen devices (2). Int J Hydrogen Energy 2021;46:11832–48.
[12] Yamabe J, Nishimura S. Influence of carbon black on decompression failure and hydrogen permeation properties of filled ethylene-propylene–diene–methylene rubbers exposed to high-pressure hydrogen gas. J Appl Polym Sci 2011;122: 3172–87.
[13] Najipoor M, Haroonabadi L, Dashti A. Assessment of failures of nitrile rubber vulcanizates in rapid gas decompression (RGD) testing: effect of physico-mechanical properties. Polym Test 2018;72:377–85.
[14] Kuang W, Arey BW, Dohnalkova AC, Kovarik L, Mills B, Menon NC, Simmons KL. Multi-scale imaging of high-pressure hydrogen induced damage in EPDM rubber using X-ray microcomputed tomography, helium-ion microscopy and transmission electron microscopy. Int J Hydrogen Energy 2023;48(23):8573–87.
[15] Jung JK, Lee CH, Baek UB, Choi MC, Bae JW. Filler influence on H2 permeation properties in sulfur-CrossLinked ethylene propylene diene monomer polymers blended with different concentrations of carbon black and silica fillers. Polymers 2022;14:592.
[16] Jung JK, Kim IG, Chung KS, Baek UB. Gas chromatography techniques to evaluate the hydrogen permeation characteristics in rubber: ethylene propylene diene monomer. Sci Rep 2021;11:4859.
[17] GridS HHIG. A systematic validation approach at various admixture levels into high-pressure grids.
[18] Lipiäinen S, Lipiäinen K, Ahola A, Vakkilainen E. Use of existing gas infrastructure in European hydrogen economy. Int J Hydrogen Energy 2023;48(23):31317–29.
[19] Birkitt K, Loo-Morrey M, Sanchez C, O'Sullivan L. Materials aspects associated with the addition of up to 20 mol% hydrogen into an existing natural gas distribution network. Int J Hydrogen Energy 2021;46:12290–9.
[20] Tetteh D. Experimental investigation of elastomer performance for underground hydrogen storage wells. 2023.
[21] Balasooriya W, Schrittesser B, Pinter G, Schwarz T. Induced material degradation of elastomers in harsh environments. Polym Test 2018;69:107–15.
[22] Ehrenstein GW, Pongratz S. Beständigkeit von Kunststoffen. München. Carl Hanser; 2007.
[23] Balasooriya W, Schrittesser B, Karunakaran S, Schlögl S, Pinter G, Schwarz T, et al. Influence of thermo-oxidative ageing of HNBR in oil field applications. Macromol Symp 2017;373:1600093.
[24] Fujiwara H, Ono H, Nishimura S. Degradation behavior of acrylonitrile butadiene rubber after cyclic high-pressure hydrogen exposure. Int J Hydrogen Energy 2015; 40:2025–34.
[25] Bhattacharjee S, Bhowmick AK, Avasthi B. High-pressure hydrogenation of nitrile rubber: thermodynamics and kinetics. Ind Eng Chem Res 1991;30:1086–92.
[26] Menon NC, Kruizenga AM, Alvine KJ, San Marchi C, Nissen A, Brooks K. Behaviour of polymers in high pressure environments as applicable to the hydrogen infrastructure. Pressure Vessels and Piping Conference: Am Soc Mech Eng 2016: V06BTA037.

[27] Yamabe J, Nishimura S. Crack growth behavior of sealing rubber under static strain in high-pressure hydrogen gas. Journal of Solid Mechanics and Materials Engineering 2011;5:690–701.
[28] Hao Y, Peng J, Zhang Z, Yang L, Gao C, Zhou F, et al. Analyzing the aging profile of serviced GIS O-ring seals under 30-year long-term field aging condition. Eng Fail Anal 2022;137:106288.
[29] Tayefi M, Eesaee M, Hassanipour M, Elkoun S, David E, Nguyen-Tri P. Recent progress in the accelerated aging and lifetime prediction of elastomers : a review. Polym Degrad Stabil 2023;214:110379.
[30] Alazhary S, Shaafaey M, Bahrololoumi A, Dargazany R. Investigation of the effect of multiple aging temperature profiles on the constitutive behavior of neoprene rubber stored in thermo-oxidative environment. ASME 2022 International Mechanical Engineering Congress and Exposition 2022. https://doi.org/10.1115/imece2022-96115.
[31] Kömmling A, Jaunich M, Goral M, Wolff D. Insights for lifetime predictions of O-ring seals from five-year long-term aging tests. Polym Degrad Stabil 2020;179:109278.
[32] Birkitt K, Loo-Morrey M, Sanchez C, O'Sullivan L. Materials aspects associated with the addition of up to 20 mol% hydrogen into an existing natural gas distribution network. Int J Hydrogen Energy 2021;46:12290–9.
[33] CSA/ANSI CHMC 2:19-Test methods for evaluating material compatibility in compressed hydrogen applications — polymers.
[34] NORSOK Standard M-710:2014-Qualification of non-metallic materials and manufacturers-Polymers.
[35] DIN EN ISO 23936-2:2011-Petroleum,petrochemical and natural gas industries – non-metallic materials in contact with media related to oil and gas production –Part 2: elastomers.
[36] Jung JK, Kim KT, Baek UB, Nahm SH. Volume dependence of hydrogen diffusion for sorption and desorption processes in cylindrical-shaped polymers. Polymers 2022;14:756.
[37] ASTM D 792. Standard test methods for density and specific gravity (relative density) of plastics by displacement. 2020.
[38] DIN EN ISO 868. Determination of indentation hardness by means of a durometer (Shore hardness). 2003 (ISO 868:2003).
[39] DIN 53504:2017-Testing of rubber-Determination of tensile strength at break, tensile stress at yield, elongation at break and stress values in a tensile test.
[40] ASTM D395-18. Standard test methods for rubber property — compression set. West Conshohocken, PA: ASTM International; 2018. www.astm.org.
[41] Din ISO 815-1:2019 - rubber, vulcanized or thermoplastic – determination of compression set – Part 1: at ambient or elevated temperatures. Beuth publisher; 2019. D, www.beuth.de.
[42] Gillen KT, Bernstein R, Wilson MH. Predicting and confirming the lifetime of o-rings. Polym Degrad Stabil 2005;87:257–70.
[43] Gillen KT, Celina M, Clough RL. Density measurements as a condition monitoring approach for following the aging of nuclear power plant cable materials. Radiat Phys Chem 1999;56:429–47.
[44] Zaghdoudi M, Kömmling A, Jaunich M, Wolff D. Scission, cross-linking, and physical relaxation during thermal degradation of elastomers. Polymers 2019;11:1280.
[45] Landi VR, Easterbrook EK. Scission and crosslinking during oxidation of peroxide cured. EPDM 1978;18:1135–43.
[46] Hassani F, Faisal NH, Nish R, Rothnie S, Njuguna J. The impact of thermal ageing on sealing performance of HNBR packing elements in downhole installations in oilfield wellhead applications. J Petrol Sci Eng 2022;208:109200.
[47] Kömmling A, Jaunich M, Wolff D. Effects of heterogeneous aging in compressed HNBR and EPDM O-ring seals. Polym Degrad Stabil 2016;126:39–46.
[48] Salehi S, Ezeakacha CP, Kwatia G, Ahmed R, Teodoriu C. Performance verification of elastomer materials in corrosive gas and liquid conditions. Polym Test 2019;75:48–63.
[49] Jaravel J, Castagnet S, Grandidier J-C, Benoît G. On key parameters influencing cavitation damage upon fast decompression in a hydrogen saturated elastomer. Polym Test 2011;30:811–8.
[50] Jeon SK, Jung JK, Chung NK, Baek UB, Nahm SH. Investigation of physical and mechanical characteristics of rubber materials exposed to high-pressure hydrogen. Polymers 2022;14:2233.
[51] Van Amerongen GJ. Influence of structure of elastomers on their permeability to gases. J Polym Sci 1950;5:307–32.
[52] Barth RR, Simmons KL, San Marchi CW. Polymers for hydrogen infrastructure and vehicle fuel systems. Livermore, CA (United States); Pacific: Sandia National Lab. (SNL-CA); 2013.
[53] Kucukpinar E, Doruker P. Molecular simulations of gas transport in nitrile rubber and styrene butadiene rubber. Polymer 2006;47:7835–45.
[54] Tan J, Chen C, Liu Y, Wu J, Wu D, Zhang X, et al. Molecular simulations of gas transport in hydrogenated nitrile butadiene rubber and ethylene–propylene–diene rubber. RSC Adv 2020;10:12475–84.
[55] Hensema ER. Polymeric gas separation membranes. Adv Mater 1994;6:269–79.
[56] Gent A, Tompkins D. Nucleation and growth of gas bubbles in elastomers. J Appl Phys 1969;40:2520–5.
[57] Gent A, Lindley P. Internal rupture of bonded rubber cylinders in tension. Proceedings of the Royal Society of London Series A Mathematical and Physical Sciences 1959;249:195–205.
[58] Koga A, Yamabe T, Sato H, Uchida K, Nakayama J, Yamabe J, et al. A visualizing study of blister initiation behavior by gas decompression. Tribol Online 2013;8:68–75.
[59] Nishimura S. Fracture behaviour of ethylene propylene rubber for hydrogen gas sealing under high pressure hydrogen. 2014.
[60] Yamabe J, koga A, Nishimura S. Failure behavior of rubber O-ring under cyclic exposure to high-pressure hydrogen gas. Eng Fail Anal 2013;35:193–205.